

## Supplementary Data

### Index

Supplementary Figure Legends	2
Supplementary Fig.1	4
Supplementary Fig.2	5
Supplementary Fig.3	6
Supplementary Fig.4	7
Supplementary Fig.5	8
Supplementary Fig.6	9
Supplementary Fig.7	10
Supplementary Table 1	11

## Supplementary Figure Legends

### Supplementary Fig.1

(a) Standard (left) and OxBiS treated Bisulfite Sequencing (BiS) profiles for a somatic male sample (46,XY SOM), female hESC line H9 (46,XX hESC) and male hESC line H1 (46,XY hESC). The region assessed by BiS analysis is the same as in Figure 1B. The methylation status of each CpG is indicated by black (methylated) and white (unmethylated), while each row is a single clone. (b) qChIP data for H3K9me3 at DXZ4 for female H9 hESC (46,XX hESC) and H9 derived EBOGs (46,XX EBOG). Each data set is graphed as a percent of input. Error bars indicate standard deviation from the mean of triplicate qPCR reactions. I-V are as in Figure 1C.

### Supplementary Fig.2

Differentiation-associated gene expression changes between hESCs and their corresponding EBOGs. (a) Quantitation of pluripotent marker gene expression in female (46,XX H9-left and H7-right) and male (46,XY H1) hESCs, female (46,XX RPE1-left and HDF-FET-right) and male (46,XY 1140) somatic cells (SOM), and female and male EBOG. Data is normalized to GAPDH expression and graphed relative to expression in H9. Error bars indicate standard deviation from the mean of triplicate qPCR reactions. (b) Indirect-immunofluorescence images showing the distribution of the indicated pluripotency markers in female (H9) hESCs (46,XX hESC), female (RPE1) somatic cells (46,XX SOM), as well as in female & male EBOG. For each sample the top row shows NANOG in green and SSEA4 in red. Nuclei are counter-stained with DAPI (white or blue). The white bars at the bottom of the merge images indicate 5 $\mu$ m. (c) Analysis of differentiation-associated gene expression in female (H9) hESCs (46,XX hESC) and their corresponding EBOGs by endpoint rtPCR analysis. Each is an inverted image of an ethidium bromide stained agarose gel.

### Supplementary Fig. 3

Characterization of transcripts around the distal EST cluster. (a) At the top is the RNA-seq profile for H1 taken from Fig. 3b and on this the area of focus is indicated, corresponding to 115,020,151-115,023,455 bp of the X chromosome (hg19). At the top is the zoomed-in RNA-seq profile for hESC H1 from the sense (+) and anti-sense strand (-) and the origins of the RNA-seq data from polyadenylated (polyA+) and nonpolyadenylated (polyA-) RNA. The y-axis is 0-300 reads. Beneath this is a schematic representation of adjacent DXZ4 monomers from the main array. The green box indicates the DXZ4 internal promoter region and the blue box the CTCF binding site. Regions of the distal EST interval showing sequence identity to DXZ4 are indicated along with the percent nucleotide identity at the top. Beneath this is the sequence verified DANT1 ATT and a DANT2 transcript inferred from EST entries BX642309 (5' read of clone DFKZp686H17267) and BX642310 (3' read of clone DFKZp686H17267). The dashed line in the open box indicates the portion of this clone that is not sequenced, whereas the solid black regions are sequence verified. Beneath this are independent unspliced EST annotations from the EST cluster. The

black arrow points to BX642310 from above. (b) Validation of the *DANT1* and *DANT2* array-traversing transcripts (ATT). A schematic representation of the DXZ4 interval is shown at the top, under which are novel ATTs identified in this study by RT-PCR, TA cloning, sequencing and mapping back to the genomic interval. Vertical lines represent exons and introns are horizontal lines with chevrons indicating the direction of transcription. The schematics correspond to the following accession numbers: (a) KM192213, (b) KM192212, (c) KM192214, (d) KM192215, (e) KM192216 and (f) KM192217. Both “a” and “b” were detected in H1 and H9 hESC, “c” was detected in H1 and H9 hESC (Figure 4) as well as CE, WB, FB, FL, HE, TR, UT, SC and ST, (d) was detected in FB, HE and UT, whereas (e) and (f) were detected in FB. Sample key, as in Fig. 4.

#### **Supplementary Fig. 4**

Expression of DXZ4 (Top) and total DANT2 (Bottom) in the 20 different human tissues assessed in Fig. 4b. Data represents qRT-PCR performed in triplicate and each is displayed as a percentage of GAPDH levels.

#### **Supplementary Fig. 5**

Detection of *DANT1*, *DANT2* and DXZ4 by direct-labeled RNA FISH probes in female H9 (top) and H7 (bottom) hESC. For each sample column 1 shows nuclei counterstained with DAPI (white), column 2 shows labeled signals indicated by arrowheads. Column 3 shows signals highlighted by arrows. Column 4 consists of a merge of the DAPI-staining (blue) with direct-RNA FISH in columns 2 (green) and 3 (red). The white bars at the bottom right of the merged images indicate 5 $\mu$ m.

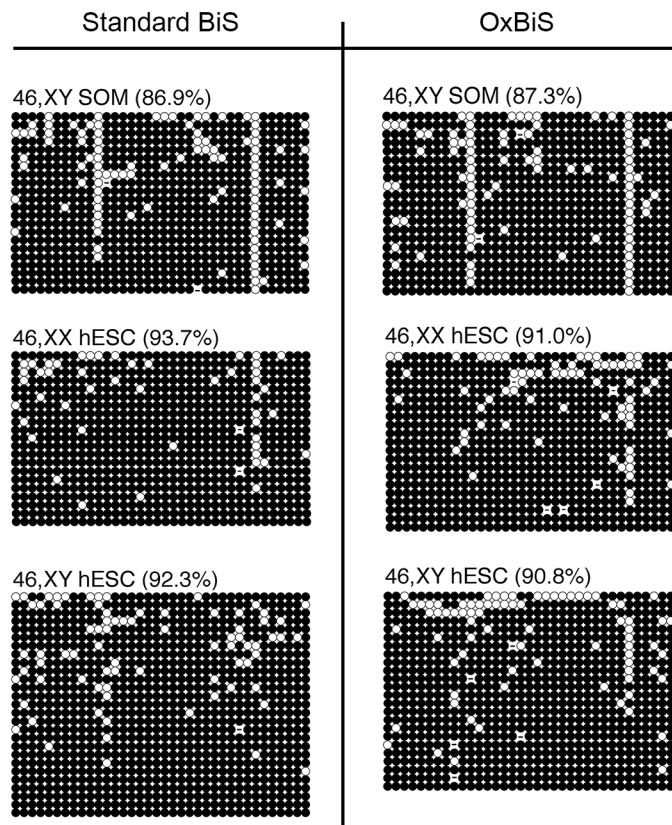
#### **Supplementary Fig. 6**

RNA and DNA FISH on RNase-treated cells. (a) RNA FISH with direct-labeled probes (*XIST*, *DANT1*, *DANT2* or DXZ4) in female (46,XX H9) and male hESCs (46,XY H1). Nuclei are counterstained with DAPI (Blue). Each panel shows data for the green or red probes to the transcripts indicated. The lack of signal is consistent with RNaseA treatment destroying the target RNA. The white bars at the bottom of the merge images indicate 5 $\mu$ m. (b) RNaseA treatment controls. Images are of 46,XX hTERT-RPE1 nuclei after RNA FISH (top row) or DNA FISH (bottom row). The probe is a spectrum-red direct-labeled DXZ4 BAC. Left images show nuclei not first treated with RNaseA, whereas right images show cells after pre-treatment with RNaseA. RNaseA treatment removes the RNA-FISH signal, but does not impact the DNA-FISH signal, confirming nucleic acid degradation is RNA specific.

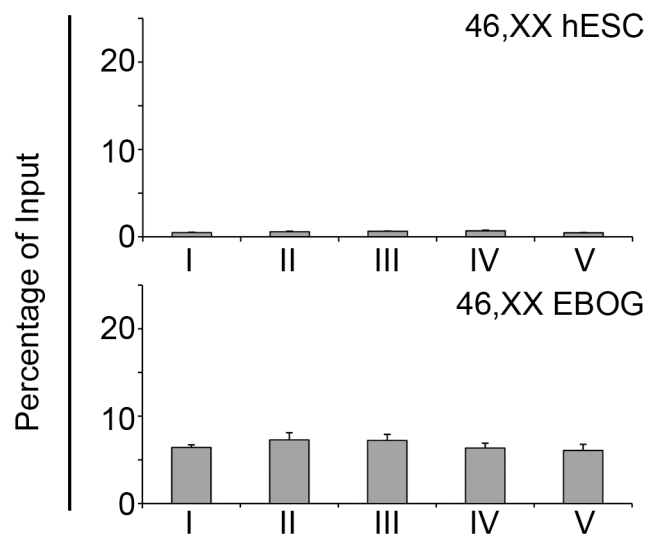
#### **Supplementary Fig. 7**

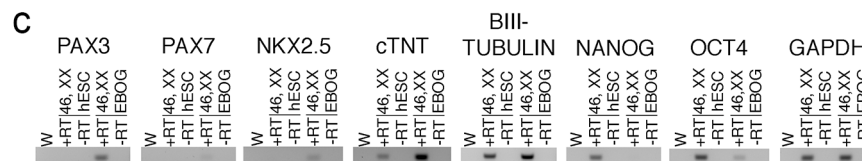
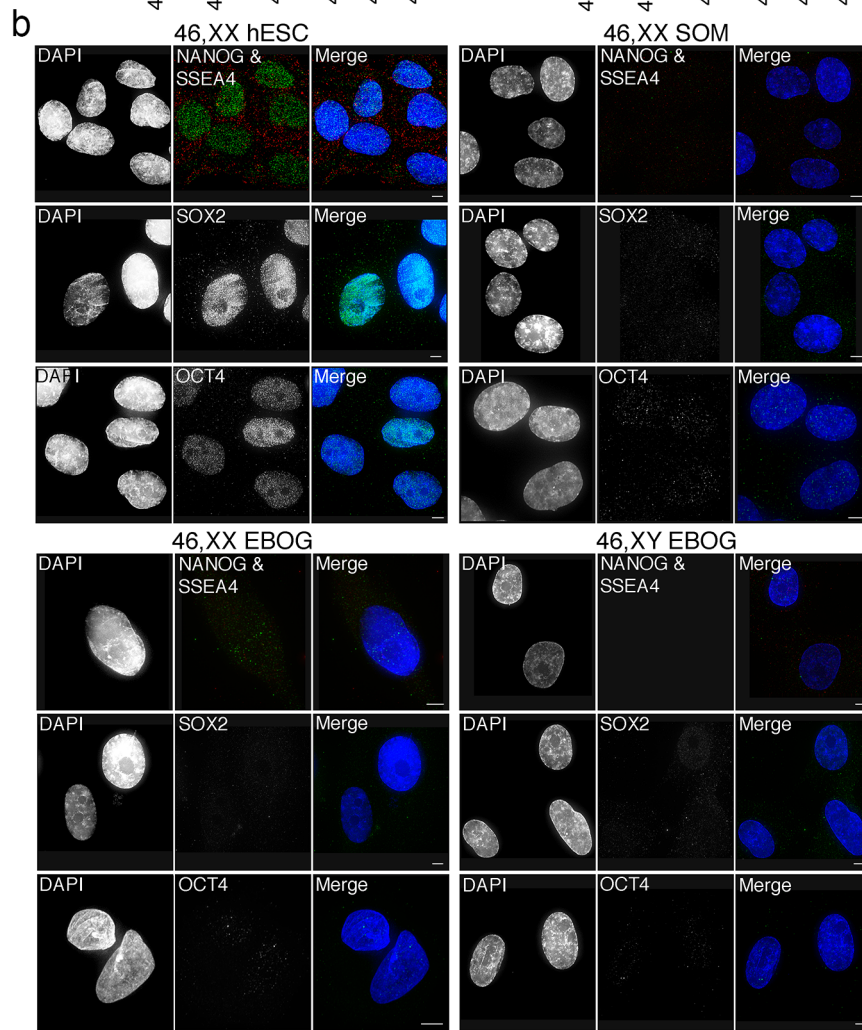
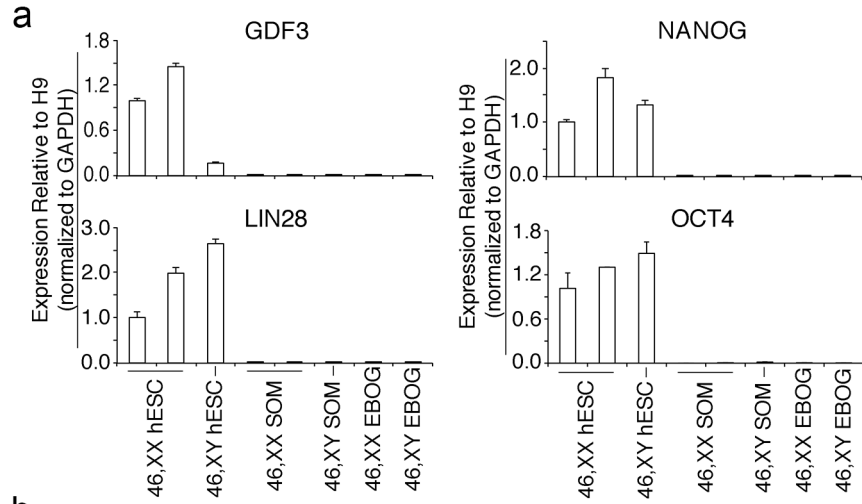
H3K9me3 qChIP data from the *DANT1* promoter region assessed at locations I (F1.R1), II (F2.R2) and III (F3.R3) as shown in Figure 6. Each is graphed as a percent of input and is the mean of triplicate qPCR reactions. Error bars indicate standard deviation. Female (46,XX) data sets are on the left with male (46,XY) on the right. For each ChIP target, the top row shows data for female (H9) and male (H1) hESCs, middle row for female (RPE1) and male (BJ1) somatic cells and bottom row for EBOGs derived from the corresponding hESCs.

a

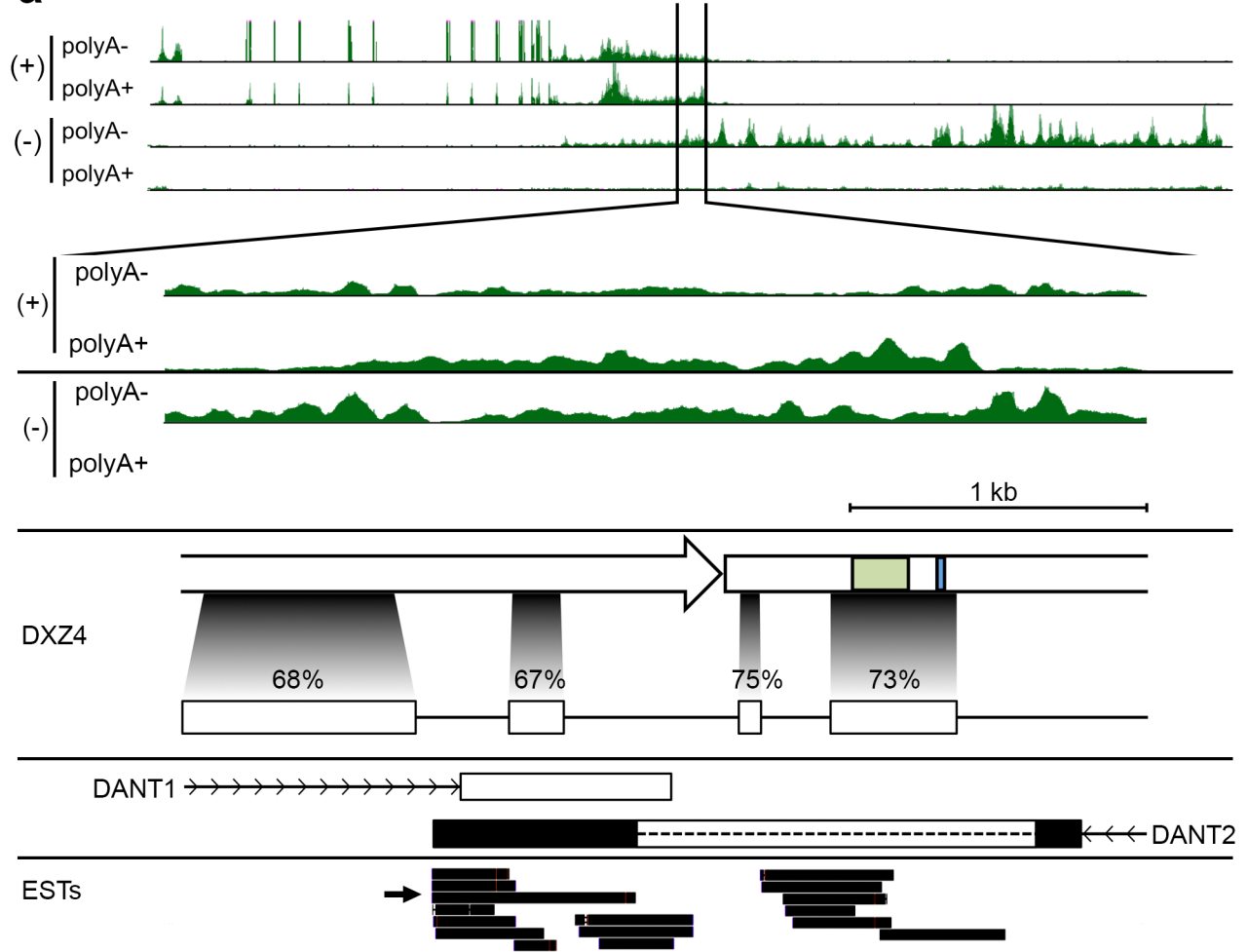


b

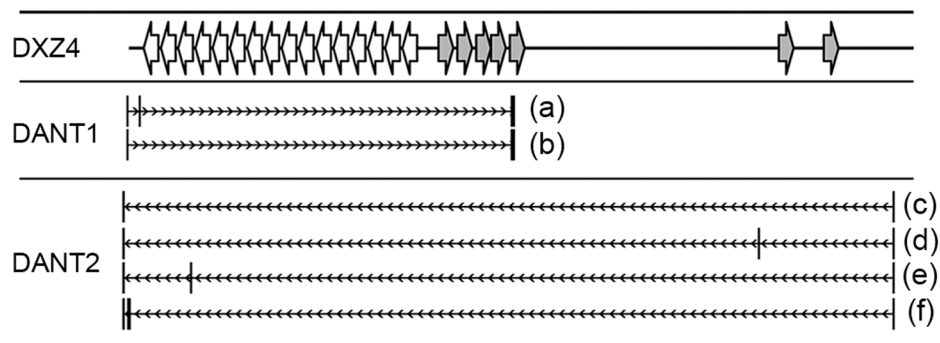


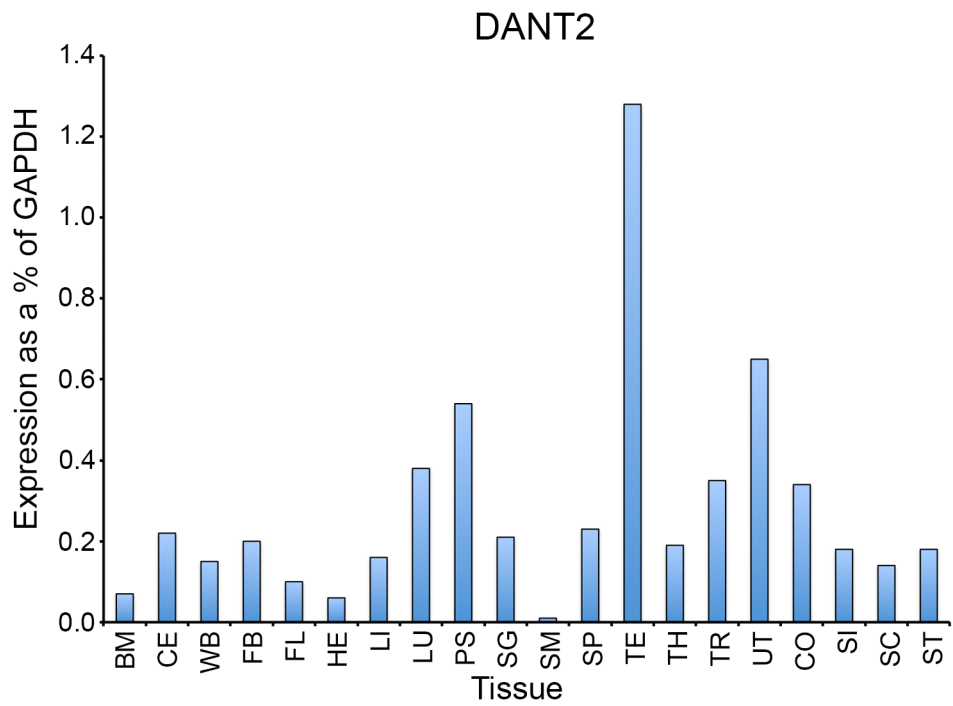
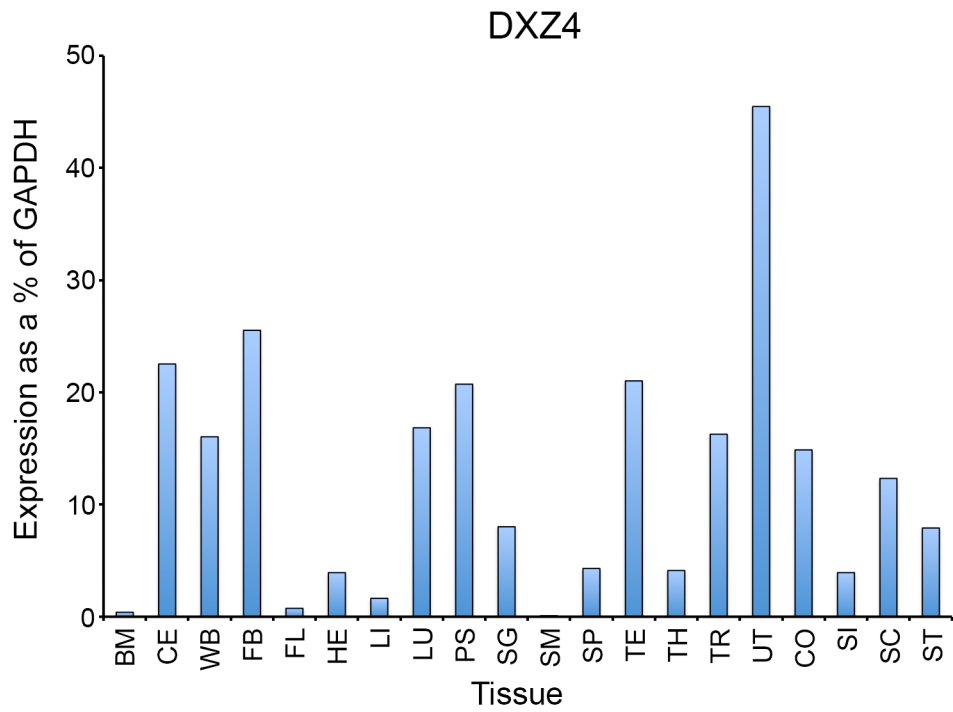


**a**

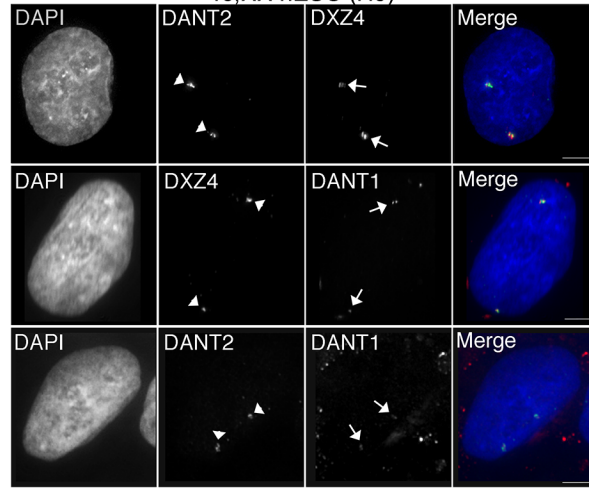


**b**

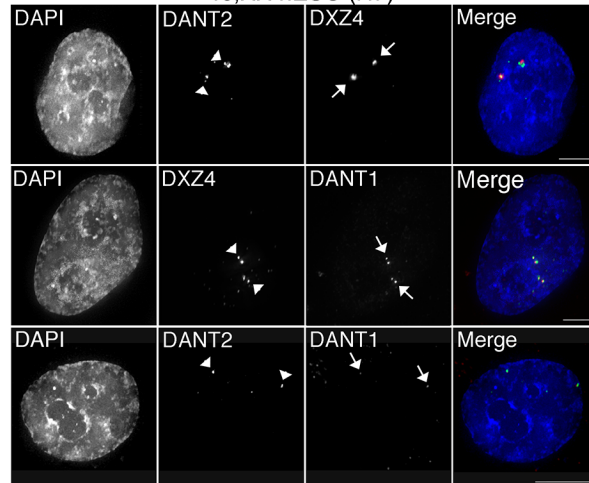




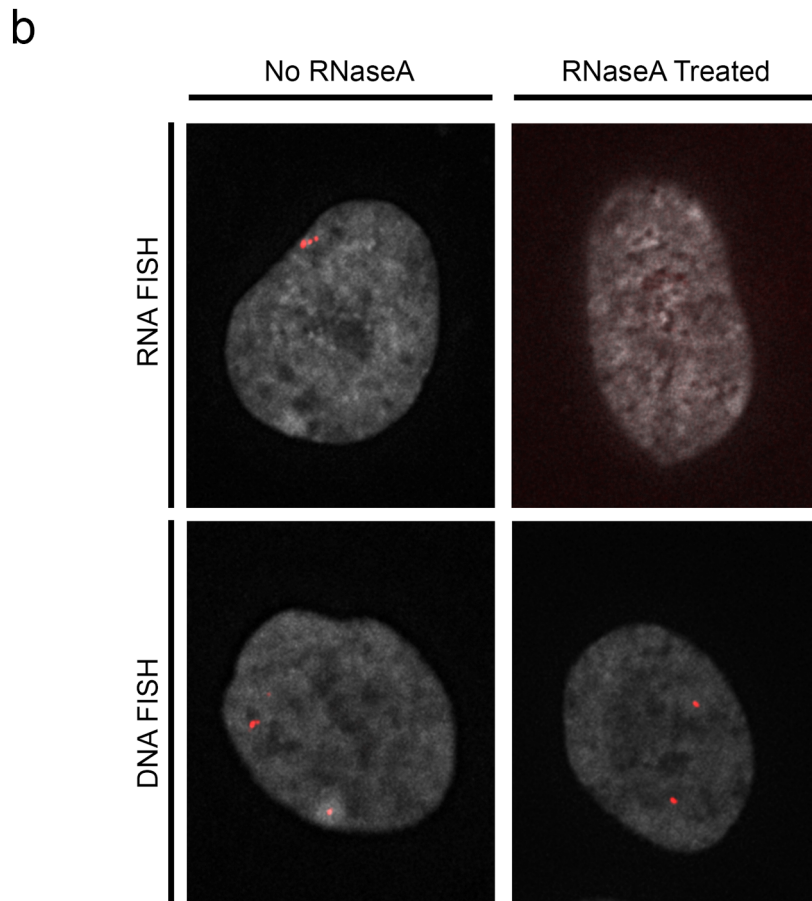
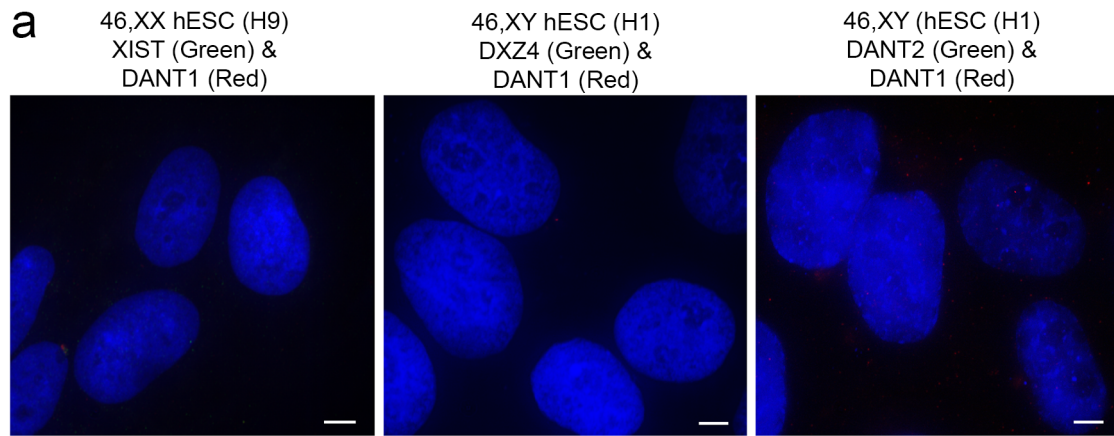
46,XX hESC (H9)

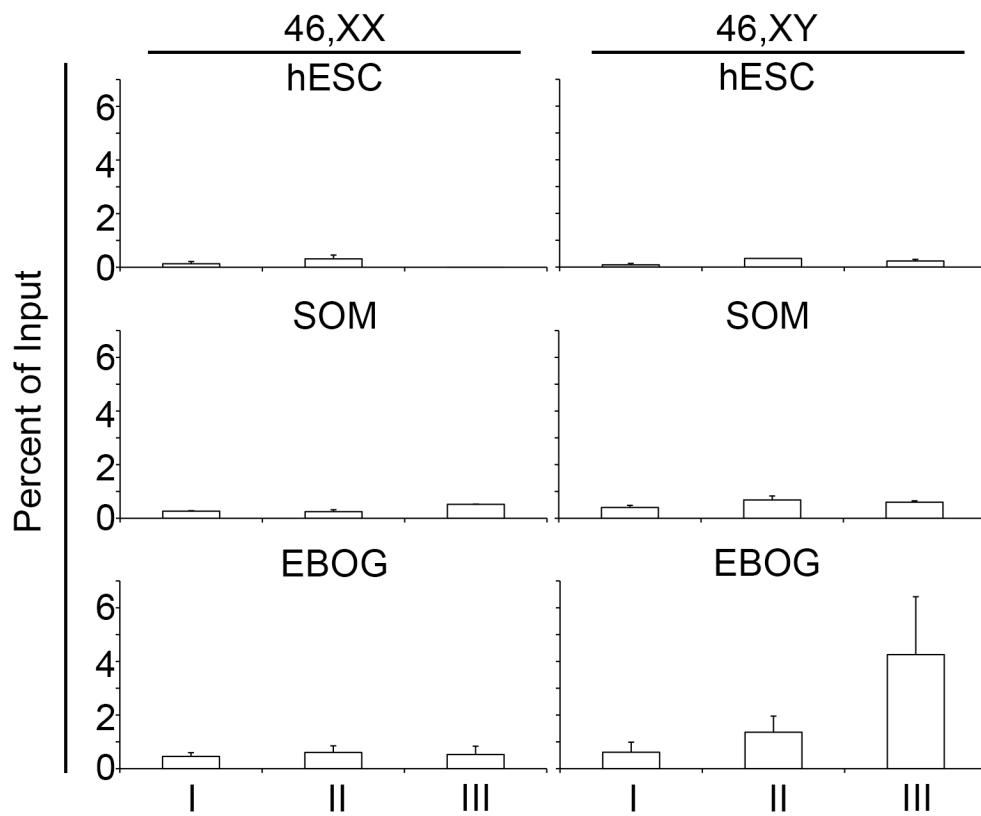


46,XX hESC (H7)









Sequence Name	Sequence 5' to 3'	Use
DXZ4-Fwd6	CAGGCAGAAATGAGCACCAC	DXZ4 qChIP- Set I
DXZ4-Rev20	TGTCCCCGAGGTTGTCTTG	DXZ4 qChIP- Set I
DXZ4-Fwd23	GGACAGTCCCAAGCCACTC	DXZ4 qChIP- Set II
DXZ4-Rev14	TCAGCAAAGGGCGGAGGG	DXZ4 qChIP- Set II
DXZ4-Fwd17	TGACCAAGAGGTCAAAGGCG	DXZ4 qChIP- Set III
DXZ4-Rev8	GTCCCGCTATTCCGGAATTG	DXZ4 qChIP- Set III
DXZ4-Fwd11	CTACGCCAAGCTGCTAACTC	DXZ4 qChIP- Set IV
DXZ4-Rev22b	CCAGCGGAAAGTZCATGGG	DXZ4 qChIP- Set IV
DXZ4-Fwd4	TAAAGGTGCGTTGACGTGG	DXZ4 qChIP- Set V
DXZ4-Rev19	GCCAGGGGGATAGGTGTG	DXZ4 qChIP- Set V
qDANT1-F1	CAGTCTCCTTTGCCCTCTTG	DANT1 qChIP- Set I
qDANT1-R1	AGTTGGGTGGGAAACCTCTT	DANT1 qChIP- Set I
qDANT1-F2	TGGCCTCAATCAGGTAGGTC	DANT1 qChIP- Set II
qDANT1-R2	AGGTCTCTGCACCAGAAAG	DANT1 qChIP- Set II
qDANT1-F3	AGAGCCTTTCTGGCCTTCC	DANT1 qChIP- Set III
qDANT1-R3	CACACCTCTCAGCCATGTAG	DANT1 qChIP- Set III
DXZ4-BiS-F1	CCAAACAAACTACCCAAAACC	BiS
DXZ4-BiS-R2	GAAGGTAGGTTAGTAAGAAGG	BiS
XIST-BiS-11F	TGGGTTAGAAAAATAAAATTAAGTAGG	BiS
XIST-BiS-11R	AATACCTACTAATTCCCTTCCCCTCTA	BiS
qrtDANT2-F1	CCTAGCTGAGGCTGCGC	qrtPCR
qrtDANT2-R1	GAGTCGCGTTGCCGCGAG	qrtPCR
qrtDANT1cd-F3	GGGCATCCTACCCCATATC	qrtPCR
qrtDANT1cd-R3	AAGGCCAGTCCGCTCTAC	qrtPCR
DANT1-Fwd	CATATCTGAGGTGCGACTGC	rtPCR; PCR-1; PCR-2
DANT1-Rev	TCACCACAGAACCTTATGTGAG	rtPCR; PCR-1
Distal ESTs-Fwd1	ATGCCCATGGCCTTGAGATG	rtPCR; PCR-4
Distal-ESTs-Rev1	GATCCAACATGGCATGTGAG	rtPCR; PCR-2
DANT2-Fwd1	AACGCAGATCAGAGGTAGTC	rtPCR; PCR-3; PCR-4; PCR-5
DANT2-Rev1	AAACCTGCGAGTCGCTGTC	rtPCR; PCR-3; PCR-6
BE297956-Rev	AACCCTAGGATCTGGAGATG	rtPCR; PCR-5
BM925596Ex2Fwd	CTTCCCAAGACCAGACACTG	rtPCR; PCR-6
GAPDH-q-Fwd	CCCAATACGACCAAATCCGT	qrtPCR
GAPDH-q-Rev	TCTCTGCTCCTCTGTTCGA	qrtPCR
GAPDH-Fwd	GAAGGTGAAGGTGCGGAGTC	rtPCR
GAPDH-Rev	GAAGATGGTGATGGGATTTTC	rtPCR
GDF3-qrt-F <sup>a</sup>	CGGGAATGTACTTCGCTTTTC	qrtPCR
GDF3-qrt-R <sup>a</sup>	CCCTTTCTTTGATGGCAGAC	qrtPCR
Lin28-qrt-F <sup>a</sup>	AAGCGCAGATCAAAGGAGA	qrtPCR
Lin28-qrt-R <sup>a</sup>	CTGATGCTCTGGCAGAAGTG	qrtPCR
totNANOG-F <sup>b</sup>	TACCTCAGCCTCCAGCAGAT	rtPCR, qrtPCR
totNANOG-R <sup>b</sup>	CCTTCTGCGTCAACACCATT	rtPCR, qrtPCR
OCT4-F1 <sup>c</sup>	CAGTGCCCGAAACCCACAC	rtPCR, qrtPCR
OCT4-R1 <sup>c</sup>	GGAGACCCAGCAGCCTCAA	rtPCR, qrtPCR
XISTqrt-F <sup>d</sup>	GAAGAGTCTCTGGCTCTTTAGAATACTGA	qrtPCR
XISTqrt-R <sup>d</sup>	CAGCGTGGTATCTTCAATGGG	qrtPCR
PAX3-F <sup>e</sup>	CTCACCTCAGGTAATGGGACT	rtPCR
PAX3-R <sup>e</sup>	CGTGGTGGTAGGTTCCAGAC	rtPCR
PAX7-F <sup>e</sup>	CCCCCGCACGGGATT	rtPCR
PAX7-R <sup>e</sup>	TATCTTGTGGCGGATGTGGTTA	rtPCR
NKX2.5-F <sup>f</sup>	TCTATCCAGGTCCACAGC	rtPCR
NKX2.5-R <sup>f</sup>	AGATCTTGACCTGCGTGGAC	rtPCR
cTNT-F <sup>f</sup>	GGCAGCGGAAGAGGATGCTGAA	rtPCR
cTNT-R <sup>f</sup>	GAGGCACCAAGTTGGGCATGAACGA	rtPCR
βIII-TUBULIN-F <sup>f</sup>	CAACAGCACGGCCATCCAGG	rtPCR
βIII-TUBULIN-R <sup>f</sup>	CTTGGGGCCCTGGGCTCCGA	rtPCR
DXZ4-DANT-F2	CGTCAGGCATACAGATGATAC	promoter construct
DXZ4-DANT-R2	CTCGGCTGCAGCCGCCATTG	promoter construct
Distal Fwd-6	GAGGTTTAAACCACTCAG	promoter construct
Distal Rev-6	GATTCTACCGAGCAACTGGC	promoter construct
FMR1-Fwd <sup>g</sup>	TGGAAGGAGGTTAAATGTTTTG	SNP sequencing
FMR1-Rev <sup>g</sup>	GGCAGAACTTCAGTTTTTACGG	SNP sequencing
MSL3-Fwd <sup>g</sup>	TGAGCAATGCTAATGGGTTG	SNP sequencing
MSL3-Rev <sup>g</sup>	ACCTGATTCATGGCACCTG	SNP sequencing
TBL1X-Fwd <sup>g</sup>	TTGGGCTTGTTGTCTCTTCC	SNP sequencing
TBL1X-Rev <sup>g</sup>	CTTACTACGCGCCAAAGTGC	SNP sequencing

<sup>a</sup>Tchieu et al. (2010) Cell Stem Cell 7:329-342

<sup>b</sup>Maherali et al. (2008) Cell Stem Cell 3:340-345

<sup>c</sup>Yu et al. (2007) Science 318:1917-1920

<sup>d</sup>Lengner et al (2010) Cell 141:872-883

<sup>e</sup>Ryan et al (2012) Stem Cell Rev and Rep 8:482-493

<sup>f</sup>Mahmood et al (2010) JMBR 25(6):1216-1233

<sup>g</sup>SNP sites from Teichroeb et al (2011) PLoS ONE 6(10):e23436